



Lawrence Berkeley Laboratory

UNIVERSITY OF CALIFORNIA

Engineering & Technical Services Division

MASTER

Presented at the 1981 International Nuclear Society,
International Symposium on Nuclear Radiation Detectors,
Tokyo, Japan, March 23-26, 1981

STATUS AND PROBLEMS OF SEMICONDUCTOR DETECTORS

Jack T. Walton, Frederick S. Goulding,
Eugene E. Haller, and Richard H. Pehl

March 1981



STATUS AND PROBLEMS OF SEMICONDUCTOR DETECTORS*

Jack T. Walton, Frederick S. Goulding, Eugene E. Haller
and Richard H. Pehl

Lawrence Berkeley Laboratory
University of California,
Department of Instrument Science and Engineering
Berkeley, California 94720

ABSTRACT

A brief review is given of the types of silicon and germanium detectors used or presently being developed for nuclear experiments. Large-area silicon and germanium detector telescopes for use in long-range particle detection and identification are emphasized. Large area position-sensitive detectors are also described.

Some results are presented regarding radiation damage and damage repair by annealing. Evidence is also presented for the importance of producing large area silicon crystals of adequate quality to reduce trapping problems to negligible proportions.

I. INTRODUCTION

The past ten years have seen a remarkable change in semiconductor radiation detectors and detector systems. High-purity germanium⁽¹⁾ has opened new applications in the gamma ray and particle telescope fields; large diameter detector grade silicon has likewise improved particle telescope and position-sensitive detector capabilities.

*This work was supported by the Director's Office of Energy Research, Division of Nuclear Physics, and by Nuclear Sciences of the Basic Energy Program, Office of Health and Environmental Research of the U.S. Department of Energy under Contract No. W-7405-ENG-48.

Spectrometers of increased resolution and complexity are in demand by experimental groups. Principal among these have been those employing the newer high intensity medium energy machines (LAMPF, SIN, Indiana and TRIUMF), or those involved in astrophysical research where weight and/or space limitations place restrictions on the spectrometers that can be employed. To these new and challenging requirements semiconductor detector spectrometers offer the possibility of energy resolutions of the order of 0.1% with wide dynamic range, light weight and moderate cost.⁽²⁾

The application and development of semiconductor detectors have been presented by several authors.^(3, 4) The applications can be broadly separated into two areas: charged-particle spectroscopy and photon spectroscopy. The considerable achievements of semiconductor detectors in light, low-energy particle spectroscopy, and in x-ray and gamma-ray photon spectroscopy are well known. In this paper we will discuss almost exclusively the status and problems of detectors used with long-range charged particles. The applications here separate almost naturally into two distinct areas; light ion intermediate energy (100 - 300 MeV) spectroscopy and relativistic heavy ion (100 - 400 MeV/amu) particle identification. We describe applications in both.

Before considering the medium-energy applications for semiconductor detectors, we note that uses exist for these devices outside the traditional nuclear science areas. For example, one of the current areas of material science analysis, Rutherford Backscattering Spectroscopy⁽⁵⁾ involves the detection of low-energy alpha (^4He) particles. Backscattering spectroscopy includes a monoenergetic beam source, scattering chamber, target assembly and associated electronics as shown in Figure 1. The alpha beam hits the target sample; the alpha particles backscattered from the target sample have an energy distribution which is uniquely correlated with the target composition to a depth of a few thousand Angstroms. This can be used to nondestructively analyze the sample. An example of RBS capabilities is shown in Fig. 2,⁽⁶⁾ where the Transmission Electron Micrograph (TEM) of a phosphorus implanted silicon wafer cross-section is shown above the backscattered spectrum from the wafer.

The silicon wafers in this example had been implanted with 120 keV phosphorous ions to a dose of $7.5 \times 10^{15}/\text{cm}^2$. Under high dose rate conditions it is possible to produce 'banding' on the wafer. These bands, which have visible colors associated with them, are regions of damage. The TEM cross

section was formed by cleaving slices from the wafer and very carefully thinning the specimens down to allow the TEM examination. The RBS spectrum was obtained by using a 1.7 MeV ^4He beam and aligning the sample so that the beam was channeled down the (1,1,1) crystal axis. The peaks labelled G_1 , G_2 and G_3 correspond to the wafer surface, and damage regions D_1 and D_2 respectively in the TEM micrograph. The regions F_1 and F_2 are relatively damage free and appear as valleys in the RBS spectrum. The damage regions are about 900 Å in width and the total depth being studied is 2500 Å. The RBS analysis is in close agreement ($\pm 5\%$) with the TEM measurements.

II. SEMICONDUCTOR DETECTOR MATERIALS AND TECHNOLOGIES

A) MATERIALS AND DETECTORS

To assist the discussion in the subsequent sections, we need to examine briefly some basic aspects of semiconductor detector technology. For this purpose, we consider a semiconductor detector to be of the form shown in Fig. 3⁽⁷⁾. Some of the physical properties of the semiconductor materials used in semiconductor detectors are listed in Table 1.⁽⁸⁻⁹⁾

Germanium and silicon have been widely used in detector fabrication. Excellent crystallinity, purity, crystal size, and extremely small trapping concentrations for charge carriers are responsible for their wide use. Germanium must be operated below 150°K to eliminate the effects of the thermally generated leakage current noise. Despite this need for cooling, germanium detectors have revolutionized the field of gamma-ray spectroscopy and more recently have begun to play an important role in charged-particle spectroscopy.

Silicon is used at room temperature in the majority of charged particle applications. For low energy (<30 keV) X-ray detection silicon must be cooled below 200°K to eliminate the leakage current noise. The small photoelectric cross-section of silicon makes it unsuitable for most gamma ray applications and its use is principally in charged particle and X-ray detection.

The compound semiconductors, cadmium-telluride (CdTe) and mercuric-iodide (HgI_2) were initially investigated as materials with high photoelectric cross-sections and a wide energy band gap which would allow, theoretically, room temperature operation of gamma ray detectors. At the present time these materials are limited to rather small areas and very thin depletion layers, and are finding applications in low-energy room temperature X-ray detection. We consider only silicon and germanium detectors in the following sections.

B) ASPECTS OF DETECTOR TECHNOLOGY

1. Detector Contacts:

The charge produced by the incident radiation in the semiconductor crystal is collected by applying an electric field, as shown in Fig. 3, across the detector. The field is produced by reverse biasing a rectifying semiconductor junction. The contacts in Fig. 3 are shown as N^+ and P^+ layers, which in fact are present only with diffused,⁽¹⁰⁾ implanted,⁽¹¹⁾ or epitaxial regrown heavily doped⁽¹²⁾ layers. Metals are also used to form rectifying contacts called Schottky barriers or surface barriers⁽¹³⁾ which for our purposes we can regard as N^+ and P^+ contacts.

Various approaches have been employed to produce thin, low leakage current contacts which will permit the application of the required electric fields (~ 1000 volts/cm) to obtain complete charge collection. Table 2 lists some of the present contact technologies in use on germanium and silicon detectors which will sustain the required fields while minimizing the bulk leakage current.

2. Surface Passivation:

Leakage currents can also be generated on the surfaces (sides in Fig. 3) of detectors. Various techniques are employed to minimize and stabilize these surface leakage currents; growth of silicon dioxide,⁽¹⁰⁾ encapsulation in epoxy, coating with special paints,⁽¹⁴⁾ deposition of insulator semiconductor films,⁽¹⁵⁾ and special shapes for the device itself.⁽¹⁶⁾ Each of these techniques has an area of application and the large number of

semiconductor detectors in use indicate that these passivation techniques are reasonably successful in controlling the surface leakage currents. In fact multiple detector particle telescopes, which form the main topic of this paper, are dependent on the availability of detectors with stable surfaces. The development of detector arrays has also been dependent on this technology.

III. MULTIPLE ELEMENT DETECTOR TELESCOPES

A) GENERAL CONSIDERATIONS

Germanium and silicon detectors with thicknesses greater than those given in Table 1 are difficult to fabricate. The energy detection properties of devices with thicknesses given in Table 1 are shown in Fig. 4 where the approximate maximum particle energy that can be stopped in the detector is plotted as a function of the atomic number of the particle.⁽¹⁷⁾ To measure longer ranged particles, a stack of detectors can be used as shown in Fig. 5. This arrangement is called a multiple-element detector telescope. In some telescopes position-sensitive detectors (drift chambers, multi-wire proportional counters, or position-sensitive semiconductor detectors) are used at the entrance to define the particle trajectory through the telescope.⁽¹⁸⁾

In applying semiconductor detectors to long-range particle detection, two factors which are usually insignificant at lower energies need to be considered: nuclear reactions and multiple scattering within the detectors. Long-range particles, have a high probability of being scattered out of the detector telescope during passage through the stack. For example, it has been calculated that a narrow beam of 200 MeV protons will spread into a beam with a standard deviation of 1 cm at the end of its approximately 10 cm track in germanium.⁽¹⁹⁾ Therefore to reduce scattering losses, tight collimation or large area detectors need to be employed. For particles having an atomic number $Z = 2$ or greater, scattering can be ignored.⁽²⁰⁾

The calculated fraction of protons undergoing nuclear reactions in silicon and germanium is shown in Fig. 6.⁽²¹⁾ The neutrons, charged particles, or

gamma rays produced by these nuclear reactions have a high probability of escaping from the detector and thereby causing a loss of signal energy. Energy is lost also in the reaction itself. For higher Z particles the nuclear reaction probability increases slowly ($\sim A^{1/3}$).

Applications for these multiple-element detector telescopes can be classified into two groups: particle spectroscopy and particle identification. Particle spectroscopy normally involves detection of one species (e.g. protons). The signals from the individual detector elements are used to reject those particles that have undergone scattering or have been involved in nuclear reactions.

In particle identifier applications, the individual signals from the detectors are combined in a particle identifier (P.I.) algorithm to determine the particle type. The procedure is an extension of earlier dual detector particle identifier algorithms.⁽²²⁾

$$P.I. = (E + \Delta E)^n - E^n \propto T M^{n-1} Z^2 \quad (1)$$

where ΔE and E are energy signals in the ΔE and E detectors, T is the ΔE detector thickness, and M , Z are the mass and charge of the particle. The exponent n is chosen so that the P.I. signal is independent of the particle energy ($M \sim 1.73$ for low-energy, low-mass particles). In a multiple detector telescope, this P.I. algorithm can be applied to various detector combinations using, for example, one detector in the stack as the ΔE detector and the remainder as the E . The identifications are compared and events which fall outside the experimental statistical range are rejected as having been involved in scattering or nuclear reactions.

To distinguish between heavy ions of only slightly different mass the particle energy loss through the telescope must be well known. This requires that thickness uniformity of the detectors be small ($< 1\%$) and that the particle trajectory through the telescope be known. Position sensitive detectors are commonly employed with these telescopes to establish the particle trajectories. Further calibration with known beams are usually employed to determine detector non-uniformities (both thickness and signal) and to establish the overall telescope performance.

B) DETECTOR CONSIDERATIONS

The availability of multiple-element particle telescopes has been dependent on specific improvements of the detector material and innovations in detector processing. High-purity germanium has made possible germanium particle telescopes. Prior to this, fabrication of germanium telescopes with lithium-compensated germanium [Ge(Li)] detectors was frustrated due to the high lithium mobility in germanium and consequent decompensation during handling of the detectors at room temperature. High-purity germanium has circumvented this problem. Further, the development of implanted N^+ and P^+ contacts ($\sim 300 - 500 \text{ \AA}$) on these detectors has yielded detectors which can be thermally annealed to remove radiation damage effects in the detector without increasing the contact thickness. This latter point is very important in application to particle identifier telescopes, since changes in the contact thickness can produce gaps in the spectrum or alter the telescope signal characteristics and thereby destroy the calibration accuracy.

Large-area silicon detector telescopes intended for long-range particle detection normally employ lithium-drifted [Si(Li)] detectors. Since standard Si(Li) detectors have N^+ contact regions of the order of 200 \mu m , for particle identifier telescopes these contacts are reduced by either lapping, or removing and replacing with a thinner lithium diffusion or with a Schottky barrier, thereby reducing or eliminating the effects of the contacts on the particle identification.⁽²³⁾

C) POSITION-SENSITIVE SEMICONDUCTOR DETECTORS

As noted earlier position-sensitive detectors (PSD's) are located at the telescope entrance to aid in heavy ion particle identification. Various techniques have been employed in making semiconductor PSD's:⁽²⁴⁾ Lamport et al⁽²⁵⁾ employed individual stripes brought out to a resistive divider, Nakamoto et al⁽²⁶⁾ employed a resistive layer with 90° contacts. The problem that these techniques are addressing is the linearization of the PSD's response. Figure 7(a) shows the equipotential lines on a resistive layer on a circular disk. The equipotential lines are actually contours of equal resistance. Consequently when employing resistive charge division to locate the position of an event, charge signals at

points Y_1 and Y_2 will give the same response. Nakamoto proposed 90° contacts to straighten these contours. Alternatively the scheme of Fig. 7(b) can be employed where conducting metal stripes (not externally connected) are evaporated onto the resistive layer thereby forcing the equipotential lines to be parallel. The resulting output position signal has the form:

$$V_{\text{out}} \propto \frac{R(Y)}{R_{\text{total}}} = \frac{\sin^{-1}\left(\frac{Y}{R}\right) + \frac{\pi}{2}}{\pi} \quad -R \leq Y \leq R \quad (2)$$

where $R(Y)$ is the resistance at the point Y along the Y -axis, R_{total} is the total resistance across the device with diameter $2R$. The response is nonlinear but can be linearized. The scheme has the advantage of avoiding the multiple contact bonding required by Lampert's approach and should be less dependent on resistive film uniformity than Nakamoto's scheme.

D) MULTIPLE-ELEMENT DETECTOR TELESCOPE PERFORMANCE

We now report on the results obtained in a few experiments that have employed large area ($\sim 10 - 15 \text{ cm}^2$) detectors in multiple-element detector telescopes.

1. Multiple-Element Particle Identifier Telescopes:

An experiment on board the ISEE-C satellite uses a silicon detector telescope consisting of ten 5 mm thick 15 cm^2 Si(Li) detectors to measure the isotopic composition of cosmic rays.⁽³⁰⁾ The telescope was designed to resolve the isotopes of Fe and this required detectors with thickness uniformity of $\pm 0.2\%$ ($\pm 10 \text{ } \mu\text{m}$) and total contact thickness of 0.3% ($15 \text{ } \mu\text{m}$). These detectors were assembled into a telescope shown schematically earlier in Fig. 5. The three pairs of X - Y drift chambers positioned at the entrance to this telescope locate particle trajectories to within 1 mm, thus allowing corrections to be made for path length variations caused by the variable entrance angles of the particles. During calibration at the BEVALAC, the scatter plot of ΔE (detectors 1 and 2) versus E (detectors 3 and 4) as shown in Fig. 8 was produced. The elements neon to iron are clearly resolved for a 230 MeV/nucleon ^{56}Fe beam and a paraffin target. In addition to resolving the elements, the isotopes are also resolved; the isotopic composition of manganese is shown in the mass histogram of Fig. 9. The mass resolution here is 0.2 amu.⁽²⁷⁾

The ISEE-C telescope has been in orbit for almost three years and has identified several anomalies in the cosmic ray composition. Some recent results obtained with this telescope are given in Fig. 10(a) which shows a scatter plot obtained from cosmic rays as measured on the satellite. This plot is comparable to the calibration data of Fig. 9. The mass histogram for the nitrogen component of the cosmic rays is given in Fig. 10(b).⁽²⁸⁾

Another area where silicon particle identifier telescopes have been employed is to study neutron rich light nuclei produced by heavy ion fragmentation.⁽²⁹⁾ The detectors in this telescope are similar to those of the ISEE-C satellite telescope, having very uniform thicknesses. As noted earlier, the detection of Fe isotopes required thickness tolerances of about $\pm 0.2\%$. The identifier capability of these telescopes is dependent on the detector uniformity. The tolerance on the thickness variations that can be allowed varies approximately as $1/Z^2$ of the incident particle, so that extension of this technique to the isotopes of elements with $Z > 26$ will be difficult.

In one fragmentation experiment conducted at the BEV/LAC, a 200 MeV/Nucleon ^{48}Ca beam with a 1 gm/cm^2 Be target was used to produce the neutron rich light nuclei. The fifteen new particle stable isotopes identified are shown in Fig. 11. The mass resolution again is approximately 0.2 amu.

2. Multiple-Element Spectroscopy Telescopes:

In many experiments involving long range particle detection where few particle species are present, the capabilities of the multiple element telescope can be employed to substantially improve the spectral resolution. In these applications the detector thickness uniformity is not as critical as with particle identification. What is important is the total stopping power of the telescope. Because of its higher stopping power, greater detector thickness, plus the capability of annealing radiation damage (either external or in situ), multiple-element germanium telescopes are finding increased use in long range particle spectroscopy. An eight-element, 10-cm^2 high-purity germanium telescope, 8.7 cm total thickness, was recently fabricated at LBL in which the detectors have ion-implanted boron and phosphorus contacts. A similar five-element telescope was recently reported by Riepe et al.⁽³⁰⁾ In this telescope

a spectral resolution of approximately 0.25% was obtained for 95 to 156 MeV protons. The beam contribution of 0.24% predominates; the detector contribution was estimated to be 0.06%.

The spectral enhancement that is possible with particle telescopes is shown in the measurements by Amann et al⁽³¹⁾ on pions. Figure 12(a) shows their results on the detection of 50 MeV pions before enhancement. The broad peak and background caused by the muons and positrons present was removed by gating on the time when the events occurred. The improvement in background in the enhanced spectrum, shown in Fig. 12(b) is evident---the spectral resolution improved from 2% unenhanced to 1% enhanced. This latter value is characteristic of the pion beam. This example illustrates that not only the energy loss measurement, but also the timing of the particle event can be employed for spectral enhancement.

E) RADIATION DAMAGE

An important consideration in the use of semiconductor detectors in particle detection is their sensitivity to radiation damage. Low-energy radiation damage has been extensively studied in both silicon and germanium detectors; germanium has been examined more extensively at higher energies.

Neutrons are a prime source of radiation damage in semiconductor detectors. A fluence of about 10^{10} neutrons/cm² will produce noticeable effects in germanium particle detectors. The deleterious effects produced by radiation damage of the semiconductor detector material are the appearance of neutral hole traps, and an increase in the ionized acceptor concentration. The hole traps cause loss of signal charge while the increase in the acceptor concentration can alter the material type. The hole traps in fast-neutron irradiated germanium detectors have been recently identified by Darken et al⁽³²⁾ as disordered regions of germanium.

The increase in the acceptor concentration in germanium detectors in a 150 MeV p(p,n) experiment at Indiana was recently documented.⁽³³⁾ High-purity germanium detector made from N-type germanium required a voltage of 1800 V for full detector depletion. During the experiment the voltage required to deplete the detector decreased indicating that the net impurity concentration $|N_D - N_A|$ in the detector was decreasing. The detector contacts would not permit application of voltages greater than 300 V beyond depletion (2100 V initially), and the

final operating voltage was 1000 V. The applied voltage was decreased throughout the experiment to maintain the 300 V over-depletion condition; the spectral resolution remained constant during the 120 hr. experiment (~ fluence of 10^9 protons/cm²). This example demonstrates that an understanding of the damage effects can allow an experiment to proceed even though the detectors are being damaged.

Procedures have been developed for annealing radiation damage in high-purity germanium. In general, the damage can be repaired by annealing the detectors for relatively short times (~ 4 hrs) at 150°C. The exact mechanism involved in this annealing process is not known, but may be associated either by recombination with vacancies and interstitials or possibly by hydrogen, which is present in the crystals, diffusing to repair the damage sites. We believe that lithium in Ge(Li) detectors performs this role and hydrogen may act in a similar fashion.

In a few cases we have observed radiation induced acceptor concentrations which could not be appreciably altered by annealing. The annealing did, however, fully restore the spectral response, so that the detectors could continue to be used. The reasons for these cases are not understood at the present time.

Silicon multiple-element telescopes employing Si(Li) detectors are generally used in low-flux experiments where few neutrons are present. However, in other areas where neutron and proton damage has been observed in individual Si(Li) detectors precipitation of the lithium at the damage sites is believed to occur. Recovery of this damage requires replacing the lithium by redrifting the device (~ 100°C, 200 V bias) for several days. With low-flux densities and long exposures, as frequently encountered in space applications, enough redrifting due to the applied bias may occur to compensate for radiation damage effects.

IV. DISCUSSION

In the preceding sections we have considered a few applications where, due to low particle flux or high probability of particle scattering, large diameter semiconductor detectors are required. The availability of material for the fabrication of these large detectors is, however, somewhat tenuous.

The development of high-purity germanium has been one of the more noted accomplishments in the detector field in the past decade. Several new analytical techniques have been developed and the physics of ultra-pure germanium has been substantially advanced.⁽³⁴⁾ Additional understanding of the purification process is still actively being pursued. For example, the concentration of carbon and carbon clusters which can cause acceptor levels in combination with hydrogen has been found to be considerably higher than was guessed previously.⁽³⁵⁾ Germanium material research has been focused on obtaining detector grade material. While material is available for large-area (60 mm diameter) detectors, the high cost (\$10 - \$20/g) is somewhat indicative of the difficulties in its production.

In contrast to germanium, there has been little research published in recent years on detector-grade silicon. Processing and economic factors have made most silicon detector manufacturers dependent on silicon sources which are closely allied with the semiconductor electronics industry. Detector grade material with diameters up to 80 mm is available, but frequently is a by-product of the normal crystal production. Optimization of the silicon crystal processing intended for the electronics industry can lead to silicon that is less perfectly suited for detector fabrication. A recent study on a few 50 mm diameter crystals where the cooling rate during crystal growth had been modified, indicated the presence of micro-impurity regions in the crystals. The modifications improved the silicon for its use in the electronics industry, but reduced the material quality for detector applications.

Research and development on the compound semiconductor materials, cadmium telluride and mercuric iodide is being conducted by a few groups. Progress in crystal improvements here has been slow but promising. The recent development of cadmium telluride crystals containing chlorine to eliminate polarization effects is indicative of the progress being made.

The semiconductor detector material situation is not as advanced as we would like. It is still evolving. However the few experiments we have described demonstrate that, with suitable material and processing, exciting results in radiation measurement can be achieved with semiconductor radiation detectors.

V. ACKNOWLEDGMENTS

We gratefully acknowledge the assistance of D.E. Greiner and T.J.M. Symons in discussions on multiple-element particle telescope performance and of M.E. Wiedenbeck in providing us with the ISEE-C satellite data and D.L. Friesei for providing the recent Indiana data. We appreciate the efforts of L. Dory for typing the manuscript.

REFERENCES

1. R.N. Hall and T.J. Soltys, IEEE Trans. Nucl. Sci. NS-18, No. 1, 160 (1971).
2. P. Siffert, Proceedings of the Topical Meeting on Intermediate Energy Physics, Zuoz, Switzerland, (1976).
3. J.M. McKenzie, Nucl. Inst. and Methods, 162, 49 (1979).
4. E.E. Haller and F.S. Goulding, Handbook On Semiconductors, Vol. 4, Ch. 6C, ed. C. Hilsum, North Holland Publ. (1980).
5. Wei-Kan Chu, J.M. Mayer and Marc A. Nicolet, Backscattering Spectrometry, Academic Press, New York (1978).
6. D.K. Sadana, M. Strathman and J. Washburn, J. Appl. Phys. 51 (11), 5718 (1980).
7. F.S. Goulding, IEEE Trans. Nucl. Sci. NS-25, No. 2, 916 (1978).
8. H.L. Malm, T.W. Raudorf, M. Martini and K.R. Zanio, IEEE Trans. Nucl. Sci. NS-20, 500 (1973).
9. R.C. Whited and M.M. Schieber, Nucl. Instr. and Methods 162, 113 (1979).
10. A.S. Grove, Physics and Technology of Semiconductor Devices, John Wiley and Sons Publ. (1967).
11. G. Dearnley, J.H. Freeman, R.S. Nelson and J. Stephen, Ion Implantation, Ch. 5, North-Holland Publ. (1973).
12. S.S. Lau and W.F. vander Weg, Thin Films Interdiffusion and Reactions, Ch. 12, Eds. J.M. Poate, K.N. Tu and J.W. Mayer, John Wiley and Sons Publ. (1978).
13. E.H. Rhoderick, Metal-Semiconductor Contacts, Ch. 2, Oxford University Press, Publ. (1978).
14. G.L. Schabale, W. Kern, R.B. Comizzoli, J. Electrochem. Soc. 122, No. 8, 1092 (1975).
15. W.L. Hansen, E.E. Haller and G.S. Hubbard, IEEE Trans. Nucl. Sci. NS-27, No. 1, 247 (1980).

16. J. Llacer, IEEE Trans. Nucl. Sci. NS-11, No. 3, 221 (1964).
17. J.F. Janni, derived from Calculations of Energy Loss, Range, Pathlength, Stragglng, Multiple Scattering and the Probability of Inelastic Nuclear Collisions from 0.1 to 1000 MeV Protons, AD-643-837, NTIS, Springfield, Va. (1966).
18. D.E. Greiner, F.S. Bieser and H.H. Heckman, IEEE Trans. Geosci. Elect. 16, 163 (1978).
19. W.M. Preston, A.M. Koehler, Radiology 104, 181 (1972).
20. D.E. Greiner, Nucl. Instr. and Methods 103, 291 (1972).
21. D.F. Measday and C. Richard-Serre, Nucl. Instr. and Methods 76, 45 (1969).
22. F.S. Goulding and B.G. Harvey, Annual Review of Nuclear Science, Vol. 25, 167 (1975).
23. J.T. Walton, H.A. Sommer, D.E. Greiner and F.S. Bieser, IEEE Trans. Nucl. Sci. NS-25, No. 1, 391 (1978).
24. E. Laegsgaard, Nucl. Instr. and Methods 162, 93 (1979).
25. J.E. Lamport, M.A. Perkins, A.J. Tuzzolino and R. Zamow, Nucl. Instr. and Methods 179, 105 (1980).
26. A. Nakamoto, K. Nagata, J. Kikuchi and T. Doke, Nucl. Instr. and Methods 130, 475 (1975).
27. M.E. Wiedenbeck, unpublished data.
28. M.E. Wiedenbeck and D.E. Greiner, The Astrophysical Journal 239, L139 (1980).
29. T.J.M. Symons, Atomic Masses and Fundamental Constants, Eds. J. Nolen and W. Benenson, 61, Plenum Press (1980).
30. G. Riepe, D. Protic, C. Sukosd, J.P. Didelez, N. Frascaria, E. Gerlic, E. Hourani, M. Morlet, to be published in Nucl. Instr. and Methods.
31. J.F. Amann, P.D. Barnes, S.A. Dytman, J.A. Penkrot, A.C. Thompson and R.H. Pehl, Nucl. Instr. and Methods 126, 193 (1975).
32. L.S. Darken, Jr., R.C. Trammell, T.W. Raudorf and R.H. Pehl, to be published in IEEE Trans. Nucl. Sci. NS-28 (1981).
33. D.L. Friesel, B. Flanders, R.H. Pehl, to be published in Nucl. Instr. and Methods.
34. E.E. Haller, W.L. Hansen and F.S. Goulding, Advances in Physics, in print.
35. E.E. Haller, W.L. Hansen and P.N. Luke, to be published in the Bulletin of the American Physical Society (1981).

FIGURE CAPTIONS

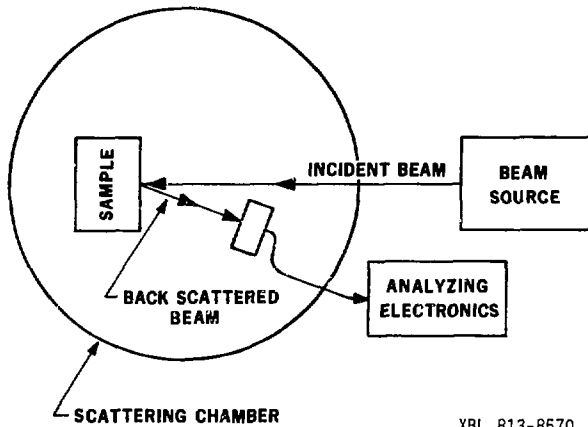
- Figure 1. Schematic arrangement of a backscattering spectrometer.
- Figure 2. Comparison of a Transmission Electron Microscope (TEM) cross section of a heavily phosphorus implanted wafer (above) and the Rutherford Backscatter Spectrum (RBS). (6)
- Figure 3. A schematic representation of a depleted semiconductor detector showing the N^+ and P^+ contacts.
- Figure 4. Maximum particle beam energy in MeV/nucleon that can be stopped in a detector of thickness X versus the particle atomic number.
- Figure 5. A multiple-element detector telescope with position sensitive drift chambers at the entrance. This is the configuration of the telescope on board the ISEE-C Satellite. (18)
- Figure 6. Percentage of protons involved in nuclear reactions in silicon and germanium as function of the incident proton energy. (21)
- Figure 7. Demonstration of the linearizing effects of metal stripes on the position response of a position-sensitive detector.
- Figure 8. $\Delta E, E$ scatter plot obtained from a 230 MeV/nucleon Fe^{56} beam with a paraffin target. Results were obtained during calibration of the ISEE-C particle telescope at the BEVALAC. The elements Ne to Fe are separated. (27)
- Figure 9. Mass histogram for manganese derived by applying a particle identifier algorithm to the data of Fig. 10. (27)
- Figure 10. (a) $\Delta E, E$ scatter plot produced by cosmic rays as measured by the ISEE-C telescope
(b) The mass histogram obtained from the data shown in (a). (28)
- Figure 11. Mass histogram of elements produced by fragmentation of a 200 MeV/nucleon ^{48}Ca beam on a Be target. The new particle stable isotopes observed in heavy ion fragmentation are $^{22}N, ^{26}F, ^{33,34}Mg, ^{35,36,37}Al, ^{38,39}Si, ^{41,42}P, ^{43,44}S$ and $^{44,45}Cl$. (29)
- Figure 12. (a) 50 MeV pion spectrum without enhancement
(b) Pion spectrum after effects of muon decay and positron escape are removed. (30)

Material	Net Impurity Concentrations $(N_A - N_D)$ ions/cc	Atomic Number		Band Gap (eV)	Hole-Electron Pair Formation Energy (eV)	Thickness Required for 90% Absorption of 60 keV γ	Planar Area Currently Available	Typical Depletion Region Width
High-Resistivity Silicon	$10^{11} - 10^{14}$	14		1.12	3.6 (300°K)	32 mm	$\leq 40 \text{ cm}^2$	$\leq 1 \text{ mm}$
Lithium-Drifted Silicon	$\sim 10^9$							$\leq 5 \text{ mm}$
High-Purity Germanium	$5 \times 10^9 - 5 \times 10^{10}$	32		0.66	2.98 (77°K)	2.2 mm	$\leq 30 \text{ cm}^2$	1-2 cm
Lithium-Drifted Germanium	$\sim 10^9$							1-2 cm
Cadmium Telluride	$\sim 10^{11}$	48	52	1.47	4.4 (300°K)	0.3 mm	$< 1 \text{ cm}^2$	$\leq 2 \text{ mm}$
Mercuric Iodide	Semi-insulator	80	53	2.13	4.2 (300°K)	0.4 mm	$< 1 \text{ cm}^2$	$\leq 1 \text{ mm}$

Table 1. Properties of Semiconductors Employed in Semiconductor Detectors(8-9)

	GERMANIUM		SILICON	
Technology	N ⁺	P ⁺	N ⁺	P ⁺
Diffusion	Lithium	-	Lithium Phosphorus, Arsenic	Boron
Implantation	Phosphorus	Boron	Phosphorus, Arsenic	Boron
Schottky Barrier	-	Nickel, Chromium Gold, Palladium	Aluminum	Palladium, Gold
Solid Phase Epitaxy	-	Aluminum Palladium, Platinum	-	Palladium, Platinum

Table 2. Contact Materials and Technology currently employed with silicon and germanium radiation detectors.



XBL 813-8570

Figure 1.

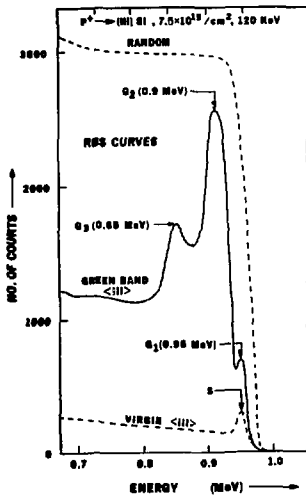


Figure 2. CBB 790-13567A

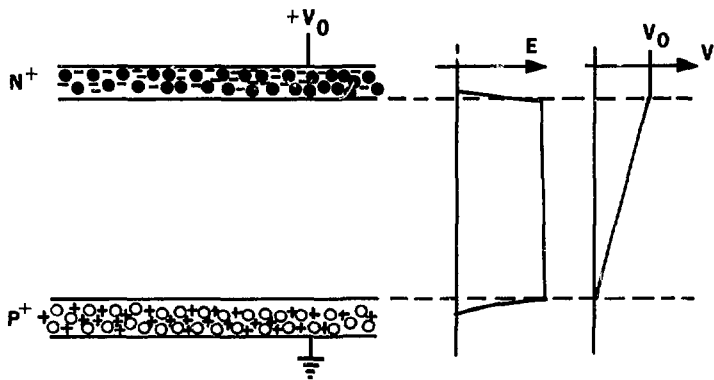


Figure 3.

XBL 7710-10299

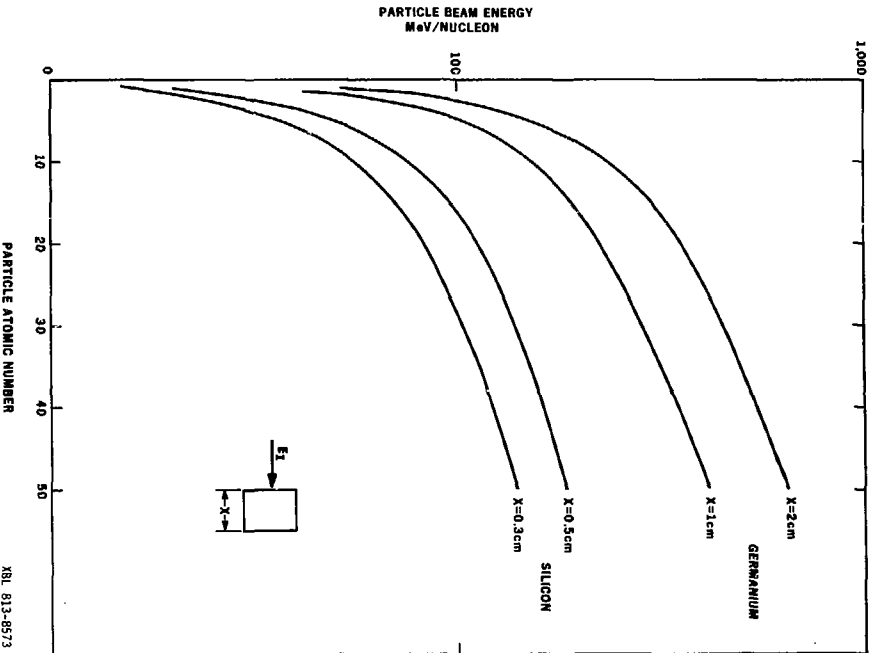


Figure 4.

XBL 813-8573

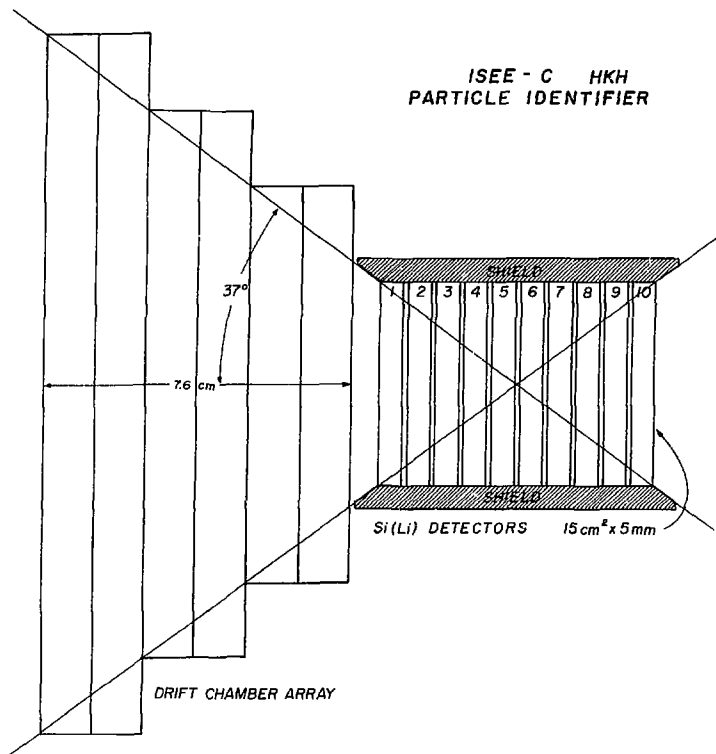


Figure 5.

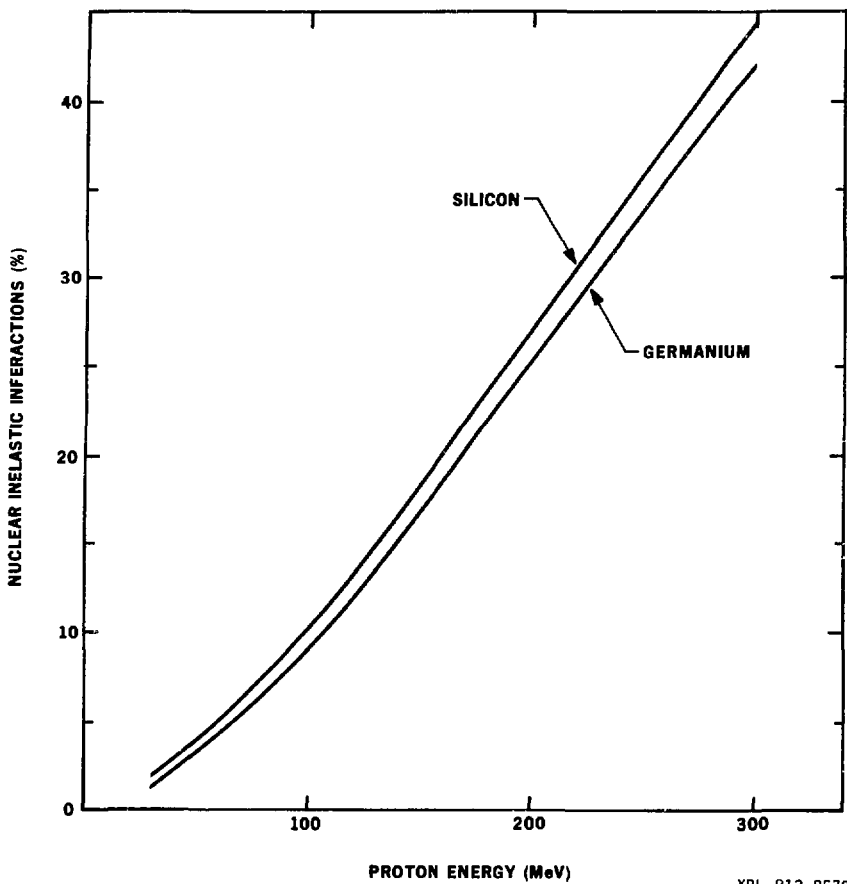
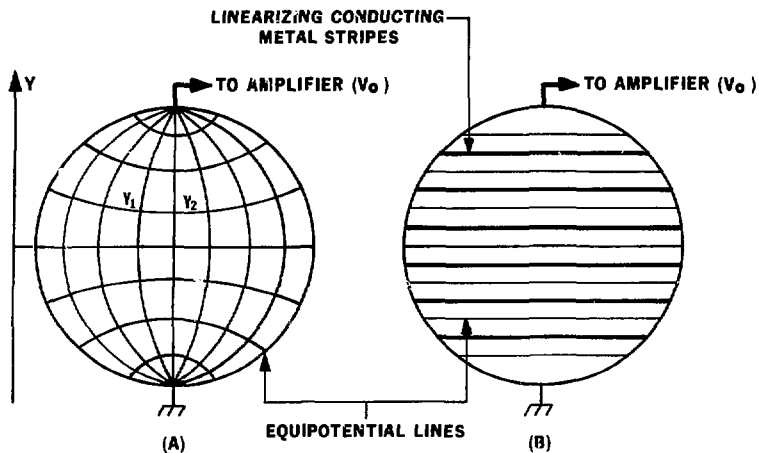


Figure 6.

XBL 813-8572



$$V_o = \frac{R\gamma}{R_{total}}$$

XBL 813-8571

Figure 7.

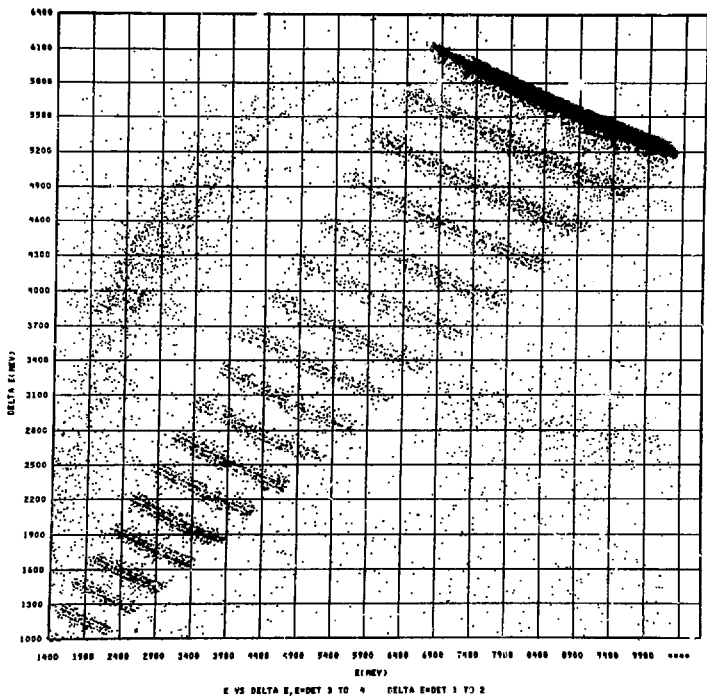


Figure 8.

XBL 788-9978

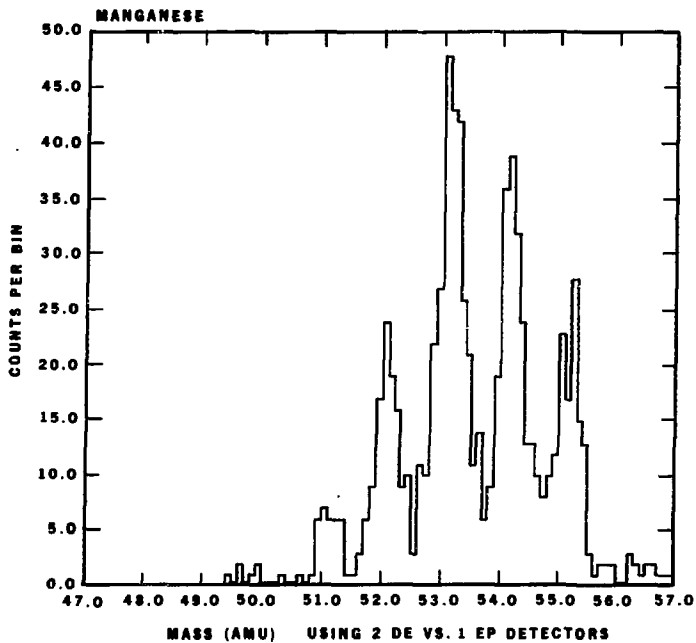
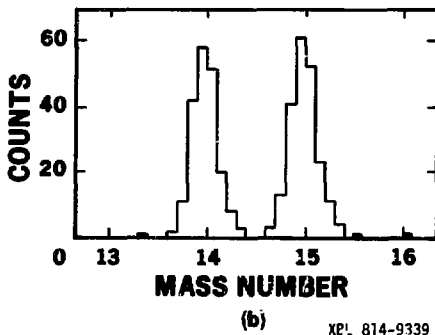
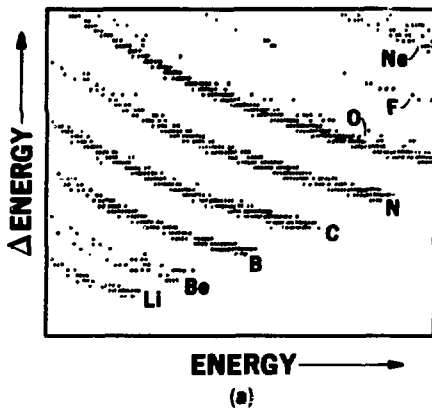


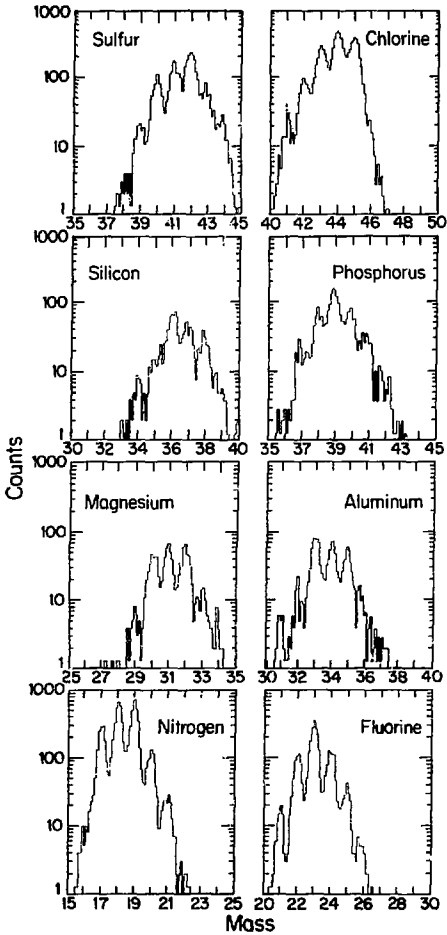
Figure 9.

XBL 792-826B



XPL 814-9339

Figure 10.



XBL 799 -2569

Figure 11.

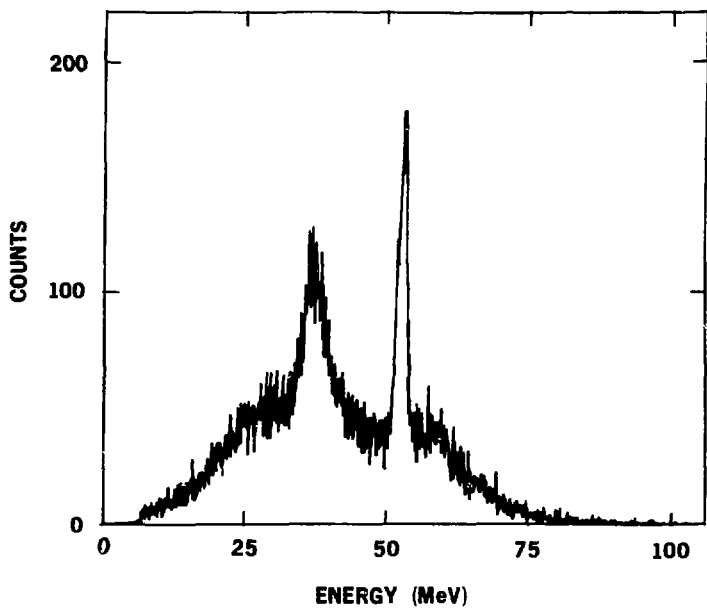


Figure 12(a).

XBL 7411-8018

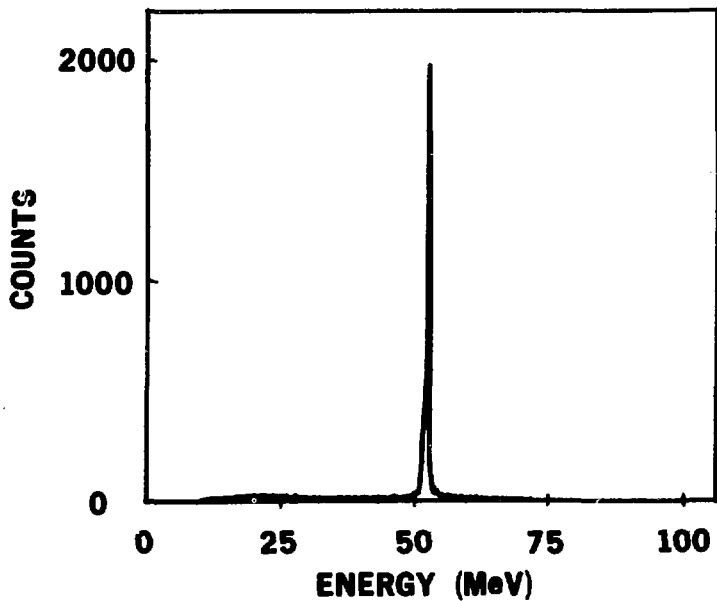


Figure 12(b).

XBL 752-316